DOI: 10.1021/cg100443d

CRYSTAL GROWTH & DESIGN Article

2010, Vol. 10
4741–4745

Supercritical Fluid−Solid Growth of Single-Crystalline Silicon Nanowires: An Example of Metal-Free Growth in an Organic Solvent

Fang-Wei Yuan and Hsing-Yu Tuan*

Department of Chemical Engineering, National Tsing Hua University, No. 101, Section 2, Kuang-Fu Road, Taiwan 30013, ROC

Received April 2, 2010; Revised Manuscript Received July 25, 2010

ABSTRACT: We report the synthesis of single-crystalline silicon nanowires on a SiO_x film-covered Si substrate in supercritical benzene without using metal nanocrystals as catalysts. Prior to synthesis, a 9 nm thick reactive SiO_x film on a silicon wafer was generated by etching a Si substrate with boiling ultrapure water, followed by annealing at 1100 °C for 30 min in Ar ambient. Si nanowires were synthesized on the 9 nm SiO_x film-covered silicon substrate at temperatures ranging from 430 to 500 °C at 1500 psi; conditions were in supercritical fluid. A large amount of Si clusters with sizes ranging from 2 to 3 nm formed in the reactive SiO_x layer, and these clusters most likely serve as nuclei for silicon nanowire growth. We refer to the SiO_x-assisted Si nanowire growth as a supercritical fluid−solid mechanism.

Introduction

Silicon (Si) nanowires have recently attracted tremendous technological interest due to their unique electrical properties, mechanical flexibility, and solution dispersibility.[1] Combined with current semiconductor manufacturing techniques, Si nanowires have been used as building blocks for the fabrication of a wide range of nanoscale devices, such as field-effect transistors, photovoltaic devices, and biological and chemical sensors.[2] Metal-seeded vapor−liquid−solid (VLS) growth has been successful to synthesize Si nanowires with precise diameter control, high aspect ratio, and low crystalline defects. In terms of reaction phases, VLS Si nanowire reactions could be categorized into gas-based routes (e.g., chemical vapor deposition (CVD), molecular beam epitaxy (MBE), and laser ablation methods) and solution-based routes (e.g., supercritical fluid−liquid−solid (SFLS) and solution−liquid−solid (SLS) methods).[3,4] Metal nanocrystals form a metal−Si liquid eutectic droplet with Si and promote the nucleation of crystalline Si nanowires from the droplet−wire interface. However, they pose various contaminations for electronic devices. For instance, gold, the most widely used metal catalyst, forms deep trap levels inside silicon and significantly diminishes the lifetime, mobility, and diffusion length of carriers in optoelectronic and electronic devices, so the use of Au is not compatible with complementary metal oxide semiconductor (CMOS) processing. To circumvent Au contamination, Ag, Al, Bi, Co, Cu, Fe, Ni, Pb, Pt, Ti, Zn, etc. were used to seed silicon nanowires due to their formation of shallower trap levels inside Si.[3] Nonetheless, a tiny metal impurity present in devices can undergo unwanted reactions, such as interaction with substrate or diffusion in silicon at high processing temperatures.[5]

Metal-seeded SFLS and SLS methods are two relatively successful solution-phase approaches for producing Si nanowires with good crystallinity and controllable diameter, in which colloidal metal nanocrystals were used to promote crystal nanowire growth via a VLS-like route. However, the use of metal nanocrystals to seed nanowires in solution suffers from more serious metal contamination problems than in vapor-phase methods. Metal nanoparticles subjected to colloid synthetic environments could easily deposit on the nanowire sidewall or thermally diffuse into growing nanowires. Moreover, purification of nanowires from products composed of a mixture of metal nanocrystals and nanowires is time-consuming and inefficient. Nonetheless, nucleation of crystalline silicon nanowires at temperatures that solvents can afford is extremely challenging due to Si's significant crystallization.[6] For example, oxide-assisted growth (OAG), a common metal-free method for silicon nanowire synthesis,[7] does not work well in the solution phase because its optimized synthetic temperature is over 1000 °C, much higher than the boiling points or decomposition temperatures of most solvents.[8] In a few cases, silicon nanowires could be synthesized by hydrothermal deposition via an OAG-like growth, but the nanowires obtained were polycrystalline and the yield was low.[9] Solution-based single-crystalline Si nanowire synthesis without metal assistance has not yet been reported.

Unsaturated silicon oxide (SiO_x) films have been studied recently as a metal alternative to catalyze growth of semiconductor nanowires, including Si, Ge, and InAs, by CVD methods.[10,11] Due to SiO_x's high reactivity, crystalline nanowires were nucleated on a reactive SiO_x film at relatively low reaction temperatures (< 600 °C). Herein we report metal-free synthesis of single-crystalline silicon nanowires in solution, using reactive SiO_x to promote Si nanowire growth on a SiO_x film-covered silicon substrate in supercritical benzene. We call this nanowire growth mechanism supercritical fluid−solid (SFS) synthesis. We also demonstrate the reliability of using the SiO_x film-covered Si substrate for SFS synthesis and extend the SFS mechanism to germanium nanowire synthesis.

Experimental Section

Chemicals. Anhydrous benzene was purchased from Sigma-Aldrich, and monophenylsilane (MPS, 97%) and diphenylgermane (DPG) were purchased from Gelest. All were stored in a nitrogen-filled box.

Experimental Details. The overall synthetic strategy is shown in Scheme 1. The procedure for preparation of a reactive SiO_x film on a

*Corresponding author. Phone: (886)3-5723661. Fax: (886)3-5715408. E-mail: hytuan@che.nthu.edu.tw.

Published on Web 10/01/2010

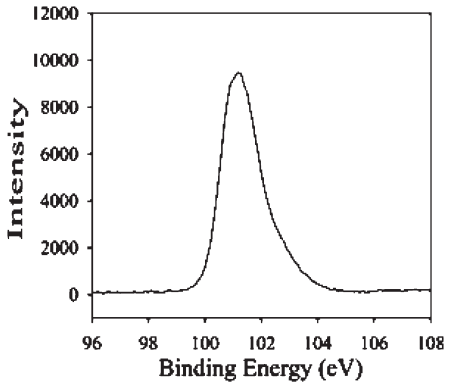

Figure 1. High-resolution Si 2p XPS of a 9 nm SiO_x film-covered substrate.

Scheme 1. Scheme for SFS Growth of Si Nanowires on a Reactive SiO_x Film-Covered Substrate

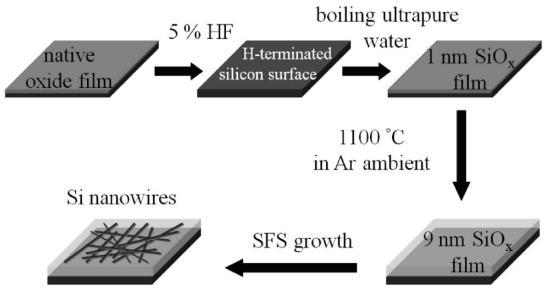

substrate is described below. A silicon wafer was chemically cleaned with acetone and etched with a diluted HF (5%) acid to remove the oxide layer. The H-terminated Si substrate was immediately etched with boiling ultrapure water for 30 min to generate a silicon oxide (SiO_x) film with a thickness of 1 nm, as confirmed by cross-section transmission electron microscopy (TEM) analysis. The thickness of the SiO_x grown is consistent with the value reported in the literature.[12] The silicon substrate coated with 1 nm SiO_x film was further annealed at 1100 °C for 30 min in Ar ambient, which increased the thickness of the SiO_x film to 9 nm. Figure 1 shows high-resolution Si 2p X-ray photoelectron spectroscopy (XPS) of a 9 nm SiO_x film-covered silicon substrate, revealing the presence of SiO_x ($0.5 < x < 1.5$) on the surface of the silicon substrate. The change in film thickness might result from oxygen diffusion from the SiO_x layer[13] or tiny oxygen contamination in the annealing furnace.[14,15] The resulting 9 nm SiO_x layer-covered silicon substrate was used for nanowire reaction. The nanowire reaction on the reactive SiO_x-covered Si substrate was carried out in a 10 mL titanium-grade reactor by a supercritical fluid−solid (SFS) process. Prior to the reaction, the reactive SiO_x film-covered Si substrate was placed into the reactor. The inlet of the reactor cell was connected to a high-pressure tubing (1/16-in. i.d.) via an LM-6 HIP reducer (High Pressure Equipment Co.). The inlet tubing was collected to a six-way valve (Valco) with a 0.5 mL injection cylinder. The reactor was covered with a heating tape, and the temperature was maintained to within ±1 °C by a temperature controller. A high-pressure liquid chromatography (HPLC) pump was used to pressurize the reactor system, and the pressure was monitored with a digital pressure gauge (Sensotech). The reactant solution was prepared in a nitrogen-filled glovebox. MPS was added to anhydrous benzene to prepare a 17 mM concentration in Si moles. In a typical nanowire reaction, the reactor was preheated to temperatures varying from 420 to 550 °C and pressurized to 800 psi. The reactant solution removed from the glovebox was injected into a 0.5 mL injection loop. The reactant mixture was injected into the reactor by the HPLC pump at a flow rate of 0.6 mL/min until reaching a final pressure of 1500 psi. After 10 min, the reactor was submerged in a water bath for 2 min and then cooled to room temperature. The reactor must be carefully opened since pressure is still present in the reactor. The Si substrate covered with as-grown nanowires was removed from the reactor and placed in an argon gas-filled glovebox for further characterization. For Ge nanowire synthesis, DPG was added to anhydrous benzene to prepare the precursor solution with a 26.5 mM concentration in Ge moles. The experimental procedure is the same as that of Si nanowire synthesis, except the reaction temperature was 370 °C.

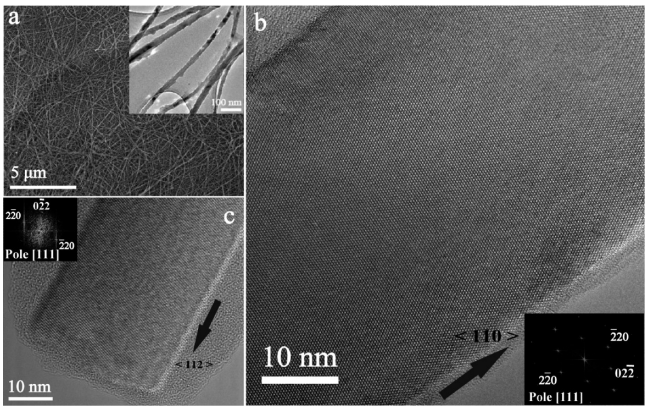

Figure 2. (a) SEM image of Si nanowires produced by decomposing MPS on a reactive SiO_x film-covered silicon substrate in supercritical benzene at 455 °C at 1500 psi. (Inset) TEM image of obtained Si nanowires, showing straight and uniform growth along the nanowire length. (b,c) HRTEM images of single-crystalline Si nanowires with (b) ⟨110⟩ and (c) ⟨112⟩ growth direction. (Insets) Corresponding indexed fast Fourier transforms of the wires.

Si Nanowires and Silicon Wafer Characterization. Nanowires were imaged by high-resolution scanning electron microscopy (SEM, Hitachi S4700 microscope) on the substrate without further purification. For LRTEM and HRTEM imaging, nanowires were either drop-casted from hexane dispersions or dry-transferred by scratching the deposition substrate onto 200-mesh lacey carbon-coated copper grids (Electron Microscope Sciences). Images were acquired using a 300 kV accelerating voltage on a JEOL JEM-3000F microscope equipped with a dispersive X-ray spectrometer. The chemical bonds of the oxide films before and after reaction were analyzed by high-resolution X-ray photoelectron spectrometry/Auger electron (HRXPS) without further treatment.

For cross-sectional observation, the silicon wafer was coated with an epoxy film and dried at 150 °C for 2 h, and then the sample was prepared by hand-polishing using different mesh sandpaper and diamond sandpaper. After polishing, the silicon substrate was contained in a copper tube of 3 mm diameter for further TEM characterization.

Results and Discussion

Figure 2a shows a SEM image of the silicon nanowire product obtained by thermally decomposing MPS in the presence of a 9 nm SiO_x layer-covered Si substrate in anhydrous benzene at 455 °C at 1500 psi, our best reaction condition. Dense Si nanowires with an average diameter of 30 nm, length > 10 μm, and a few dislocation defects were obtained. HRTEM images of as-synthesized Si nanowires (Figure 2b,c) show that these nanowires are single-crystalline. Wires were coated with a thin (< 2 nm), rough, amorphous layer composed of silicon, carbon, and oxygen as confirmed by energy-dispersive X-ray spectroscopy (EDS), which might be attributed to reaction byproducts such as polymeric phenylsilane coating.[16] Most of the obtained Si nanowires exhibit predominantly ⟨110⟩ and ⟨112⟩ directions (Figure 2b,c and Supporting Information, Figure S1), which are most likely the result of minimization of the surface energy of the nanowires.[17] Raman spectrum of the product demonstrates good crystallinity of Si nanowires (Supporting Information, Figure S2).[18]

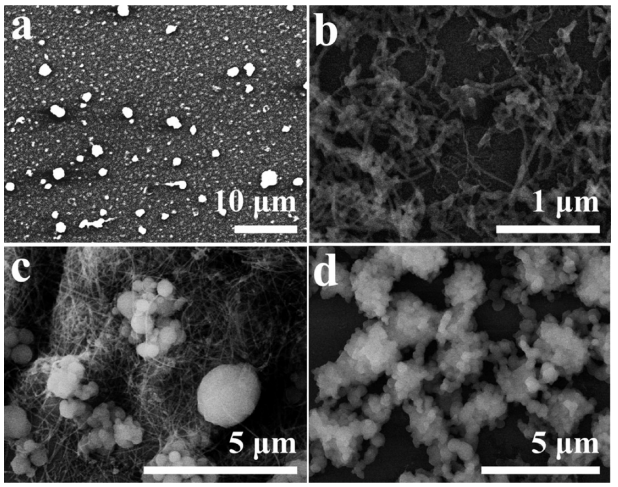

Figure 3. SEM images of Si nanowires grown at (a) 400, (b) 440, (c) 470, and (d) 500 °C.

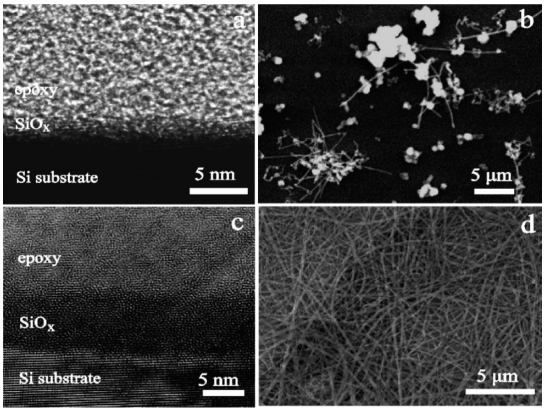

Figure 4. (a) Cross-section TEM image of a Si substrate etched with boiling ultrapure water for 30 min, showing a 1 nm SiO_x layer covered on the substrate. (b) SEM image of Si nanowire product using the Si substrate of (a). (c) Cross-section TEM image of annealing the silicon substrate of (a) at 1100 °C for 30 min in Ar ambient. (d) SEM image of Si nanowire product using the Si substrate of (c).

As shown in Figure 3, the nanowire synthesis is very sensitive to reaction temperature. At temperatures below 400 °C, small amounts of spherical particles with diameters of hundreds of nanometers were grown on a silicon substrate, showing that Si prefers isotropic growth rather than anisotropic nanowire growth at relatively low temperatures (Figure 3a). This result reveals that Si nanowire growth requires sufficient thermodynamic energy to enable apparent precursor decomposition and their one-dimensional growth. At temperatures between 400 and 440 °C, although nanowires could be obtained, they were curly and short, and wire crystallinity was poor (Figure 3b). This result indicates that the thermodynamic energy in this temperature range is still not sufficient to achieve optimal nanowire growth. At temperatures between 470 to 500 °C, the kinetics of Si particle nucleation appears to compete with that of nanowire growth. Straight and long nanowires were synthesized, but there also appeared to be a large amount of particulate byproduct (Figure 3c). At reaction temperatures exceeding 500 °C, only micrometer-sized Si particles formed (Figure 3d), which shows that the rate of homogeneous reaction of Si overwhelms the nanowire crystallization rate and results in only large Si particles as the product. The thickness of the SiO_x film has a significant influence on the reaction result. Although Si nanowires could be grown on a 1 nm SiO_x layer-covered Si substrate (Figure 4a,b), the yield of nanowires was low and the quality was poor. Much better quality nanowires were obtained on a 9 nm thick SiO_x layer-covered substrate (Figure 4c,d), showing that sufficient SiO_x is required to enable Si nanowire growth (see Supporting Information, Figure S3, for TEM images of a larger area of SiO_x layer). We also conducted reactions in the presence of a native oxide film-covered Si substrate as a control experiment, and no wires but only amorphous Si particles formed, showing that nanowire growth must be carried out on a reactive SiO_x film-covered substrate (Supporting Information, Figure S4).

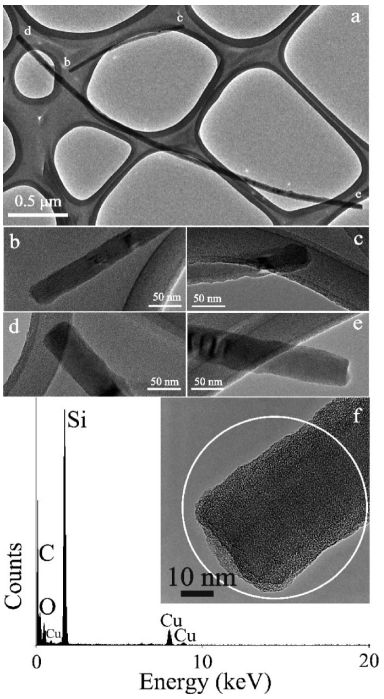

Figure 5. (a) TEM image of two Si nanowires showing both ends. (b–e) TEM images taken at the ends of the Si nanowires in (a). (f) EDS taken at the ends of the nanowire, showing the composition to be Si; any O is from Si surface oxidation, and the Cu signal is from the copper TEM grid.

To confirm that no metals or other impurities were involved in the nanowire growth, the following characterizations were conducted. First, the ends of the nanowires did not attach to any metal seeds or other carbonaceous droplets which might induce nanowire growth. Figure 5a shows two silicon nanowires at a lower magnification with both ends imaged. Closer imaging of the ends of the two wires again shows a clean surface with no impurity (Figure 5b–e). Second, EDS analysis of both the wire body and the ends shows that the major component is Si; the Cu signal is from background scattering off the copper grid, O is from oxygen on the Si surface, and C is from MPS decomposition byproduct and the carbon-coated copper grid (Figure 5f). Finally, prior to and after nanowire reaction, XPS was conducted on a silicon substrate to detect the presence of eight different metals, Au, Al, Fe, Ni, Ti, Cu, Pb, and Zn (Supporting Information, Figure S5), which could promote Si nanowire growth. The detected signals of these metals are all less than 0.1 ppm (Supporting Information, Table S1), thus excluding the possibility of metal impurity in our system.

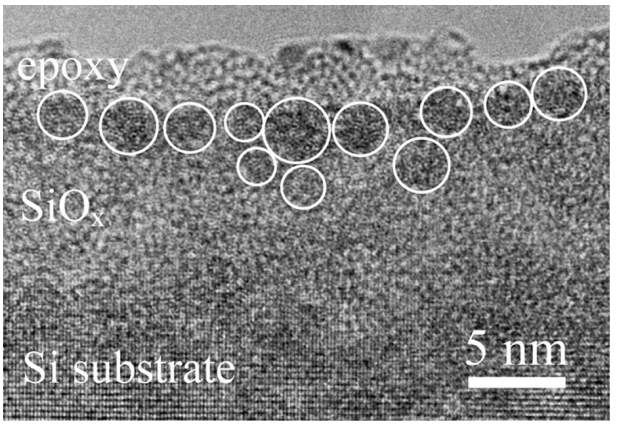

Figure 6. Cross-section TEM image of a SiO_x film-covered Si substrate after thermal decomposition of MPS in anhydrous benzene at 455 °C and 1500 psi. The circled areas shows the silicon-rich clusters which are embedded inside the SiO_x film.

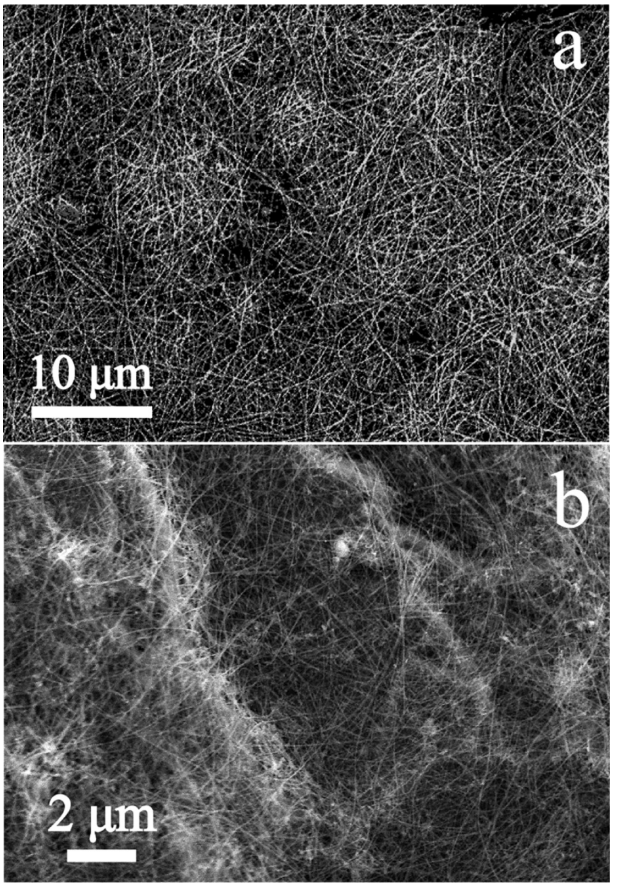

Figure 7. SEM images of Si nanowires synthesized on the same Si substrate on the (a) third and (b) sixth reuses. Before each reuse reaction, the substrate was first treated with the wire removal process, followed by a two-step SiO_x film generation procedure.

The nanowire growth mechanism could be described as a SFS growth scheme. Thermal decomposition of phenysilanes undergoing homogeneous bimolecular disproportionation reactions between phenylsilane molecules leads to silane and diphenylsilane via a four-center activated complex at temperatures above 400 °C, as studied in both the gas phase and the solution phase.[19] The silane from MPS disproportion might be adsorbed onto the reactive SiO_x surface and form

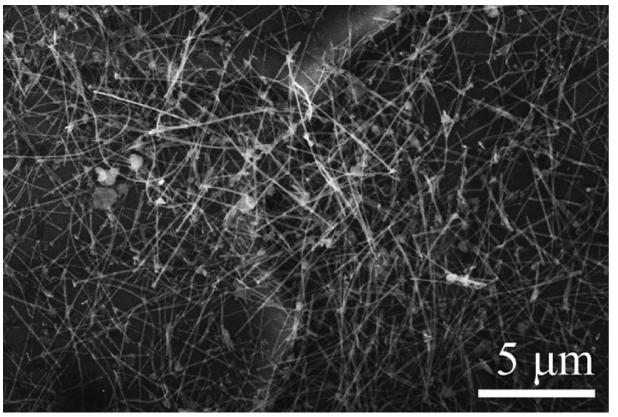

Figure 8. SEM image of Ge nanowires grown on a 9 nm SiO_x layer-covered Si substrate.

the catalytic sites that are critical for Si nanowire growth. We conducted cross-section TEM imaging of a silicon substrate after nanowire reaction to image products near the SiO_x film. A large amount of Si clusters with sizes ranging from 2 to 3 nm were found to be embedded near the SiO_x layer (Figure 6). Since SiO_x becomes unstable at temperature above 400 °C,[20] silane might dissociate readily into the SiO_x and yield cluster-like Si. This result shows that the SiO_x-assisted nanowire growth mostly like involves such cluster-like Si at the beginning of wire growth. We speculate that these Si clusters serve as nuclei for further anisotropic growth of nanowires. After Si supersaturation from continued feeding, Si nanowires grow outward from the SiO_x-covered surface, as shown in Supporting Information, Figure S6. We propose that the SiO_x film most likely takes over the "catalyst" function in the SFS nanowire growth. It should be noted that the thickness of SiO_x remains unchanged after the nanowire reaction, indicating that the SiO_x layer plays the function of a catalytic bed to incubate the formation of these Si clusters. Without the presence of SiO_x film, thermal decomposition of MPS yielded only microsized amorphous Si particles due to the absence of Si nuclei for nanowire growth. The SiO_x film's crucial role has also been observed in other SiO_x-assisted semiconductor nanowire syntheses by CVD methods.[11] After removal of wires from the substrate, the same Si substrate could be reused for SFS nanowire synthesis by repeated treatment with the two-step SiO_x film generation procedure. Figure 7a,b shows SEM images of Si nanowires synthesized on the same silicon substrate after third and sixth film generation treatment, respectively. Nanowire quality has no observable difference in each batch, demonstrating the reliability of utilizing SiO_x for SFS nanowire growth.

We also apply the SiO_x-assisted SFS growth mechanism for Ge nanowire synthesis. Figure 8 shows the SEM image of Ge nanowires obtained from nanowire reaction at 370 °C at 1500 psi. The lower synthesis temperature is due to the relatively lower temperature required for DPG decomposition and the lower energy required for Ge crystallization. Detailed studies of the SiO_x-assisted Ge nanowire synthesis are in progress.

Conclusion

We have successfully presented a method to synthesize single-crystalline Si nanowires without any metal catalysts in supercritical benzene. Reactive SiO_x is an effective catalyst to foster Si nanowire growth via a supercritical fluid−solid

growth mechanism. We also demonstrate the reliability of using SiO_x as a catalytic medium for Si nanowire growth. We have extended this SiO_x-assisted SFS growth to Ge nanowire synthesis. We believe that this approach could also be extended to the synthesis of other compound semiconductors, such as InAs and InP nanowires, in supercritical fluid or other kinds of solution-based semiconductor nanowire synthesis (i.e., hot-boiling-point solvent synthesis). The study reported here provides a new solution to metal contamination problems for solution-phase semiconductor nanowire synthesis as well as a new growth scheme for solution-based Si nanowire synthesis.

Acknowledgment. The authors gratefully acknowledge financial support from the National Tsing Hua University start-up fund and Booster Program (97N2561E1), CGMH-NTHU Joint Research Program (CMRPG380011), and National Science Council (NSC 97-2218-E-007-007 and NSC 98-2221-E-007-075), Taiwan.

Supporting Information Available: Raman spectrum, SEM and TEM images of wires, and cross-section TEM images and XPS of a reactive SiO_x film-covered substrate before and after nanowire reaction. This material is available free of charge via the Internet at http://pubs.acs.org.

References

(1) (a) Yin, Y. D.; Gates, B.; Xia, Y. N. *Adv. Mater.* **2000**, *12*, 1426–1430. (b) Korgel, B. A. *AIChE J.* **2009**, *55*, 842–848. (c) Wu, X.; Kulkarni, J. S.; Collins, G.; Petkov, N.; Almcija, D.; Boland, J. J.; Erts, D.; Holmes, J. D. *Chem. Mater.* **2008**, *20*, 5954–5967. (d) Lee, S. T.; Peng, H. Y.; Zhou, X. T.; Wang, N.; Lee, C. S.; Bello, I.; Lifshitz, Y. *Science* **2000**, *287*, 104–106.

(2) (a) Tian, B. Z.; Zheng, X. L.; Kempa, T. J.; Fang, Y.; Yu, N. F.; Yu, G. H.; Huang, J. L.; Lieber, C. M. *Nature* **2007**, *449*, 885–889. (b) Yang, C.; Zhong, Z. H.; Lieber, C. M. *Science* **2005**, *310*, 1304–1307. (c) Xiang, J.; Lu, W.; Hu, Y. J.; Wu, Y.; Yan, H.; Lieber, C. M. *Nature* **2006**, *441*, 489–493. (d) Hochbaum, A. I.; Fan, R.; He, R. G.; Yang, P. D. *Nano Lett.* **2005**, *5*, 457–460.

(3) (a) Arnold, D. C.; Hobbs, R. G.; Zirngast, M.; Marschner, C.; Hill, J. J.; Ziegler, K. J.; Morris, M. A.; Holmes, J. D. *J. Mater. Chem.* **2009**, *19*, 954–961. (b) Kuno, M. *Phys. Chem. Chem. Phys.* **2008**, *10*, 620–639.

(4) (a) Schmidt, V.; Wittemann, J. V.; Senz, S.; Gosele, U. *Adv. Mater.* **2009**, *21*, 2681–2702. (b) Schmidt, V.; Wittemann, J. V.; Gosele, U. *Chem. Rev.* **2010**, *110*, 361–388.

(5) Murarka, S. P. *Silicides For Vlsi Applications*; Bell Telephone Laboratories: New York, 1983.

(6) (a) Hessel, C. M.; Henderson, E. J.; Veinot, J. G. C. *J. Phys. Chem. C* **2007**, *111*, 6956–6961. (b) Zhang, X. M.; Neiner, D.; Wang, S. Z. *Nanotechnology* **2007**, *18*, 095601. (c) Kang, K.; Gu, G. H.; Kin, D. A.; Park, C. G.; Jo, M. H. *Chem. Mater.* **2008**, *20*, 6577–6579.

(7) Zhang, R. Q.; Lifshitz, Y.; Lee, S.-T. *Adv. Mater.* **2003**, *15*, 635–640.

(8) Lee, D. C.; Mikulec, F. V.; Korgel, B. A. *J. Am. Chem. Soc.* **2004**, *126*, 4951–4957.

(9) Tang, Y. H.; Pei, L. Z.; Lin, L. W.; Li, X. X. *J. Appl. Phys.* **2009**, *105*, 044301.

(10) Kim, B. S.; Koo, T. W.; Lee, J. H.; Kim, D. S.; Jung, Y. C.; Hwang, S. W.; Choi, B. L.; Lee, E. K.; Kim, J. M.; Whang, D. *Nano Lett.* **2009**, *95*, 864–869.

(11) Mandl, B.; Stangl, J.; Martensson, T.; Mikkelsen, A.; Eriksson, J.; Karlsson, L. S.; Bauer, G.; Samuelson, L.; Seifert, W. *Nano Lett.* **2006**, *6*, 1817–1821.

(12) Morita, M.; Ohmi, T.; Kawakami, H. M.; Suma, K. *Appl. Phys. Lett.* **1989**, *55*, 562–564.

(13) Jud, E.; Tang, M.; Chiang, Y. M. *J. Appl. Phys.* **2008**, *103*, 114108.

(14) Hirmke, J.; Rosiwal, S. M.; Singer, R. F. *Vacuum* **2008**, *82*, 599–607.

(15) Datta, S.; Cohen, J. D.; Golledge, S. L.; Xu, Y.; Mahan, A. H.; Doyle, J. R.; Branz, H. M. *Mater. Res. Soc. Symp. Proc.* **2006**, *910*, 0910–A02−05.

(16) Chan, C. K.; Patel, R. N.; O'Connell, M. J.; Korgel, B. A.; Cui, Y. *ACS Nano* **2010**, *4*, 1443–1450.

(17) (a) Wu, Y.; Cui, Y.; Huynh, L.; Barrelet, C. J.; Bell, D. C.; Lieber, C. M. *Nano Lett.* **2004**, *4*, 433–436. (b) Zhang, Y. F.; Tang, Y. H.; Wang, N.; Lee, C. S.; Bello, I.; Lee, S. T. *Phys. Rev. B* **2000**, *61*, 4518–4521.

(18) Liu, L. Z.; Wu, X. L.; Zhang, Z. Y.; Li, T. H.; Chu, P. K. *Appl. Phys. Lett.* **2009**, *95*, 093109.

(19) (a) Tuan, H. Y.; Korgel, B. A. *Chem. Mater.* **2008**, *20*, 1239–1241. (b) Coutant, R. W.; Levy, A. *U.S., Aerosp. Res. Lab.,* [*Rep.*] **1969**, *69*, 0213. (c) Gilman, H.; Miles, D. H. *J. Org. Chem.* **1958**, *23*, 326–328. (d) Speier, J. L., Jr.; Zimmerman, R. E. *J. Am. Chem. Soc.* **1955**, *77*, 6395–6396. (e) Russell, G. A. *J. Am. Chem. Soc.* **1959**, *81*, 4815–4825.

(20) Wang, J.; Wang, X. F.; Li, Q.; Hryciw, A.; Meldrum, A. *Philos. Mag.* **2007**, *87*, 11–27.